Chapter 5

Creation of Long-Acting Nanoformulation for Delivery of Cationic Hydrophilic Drug

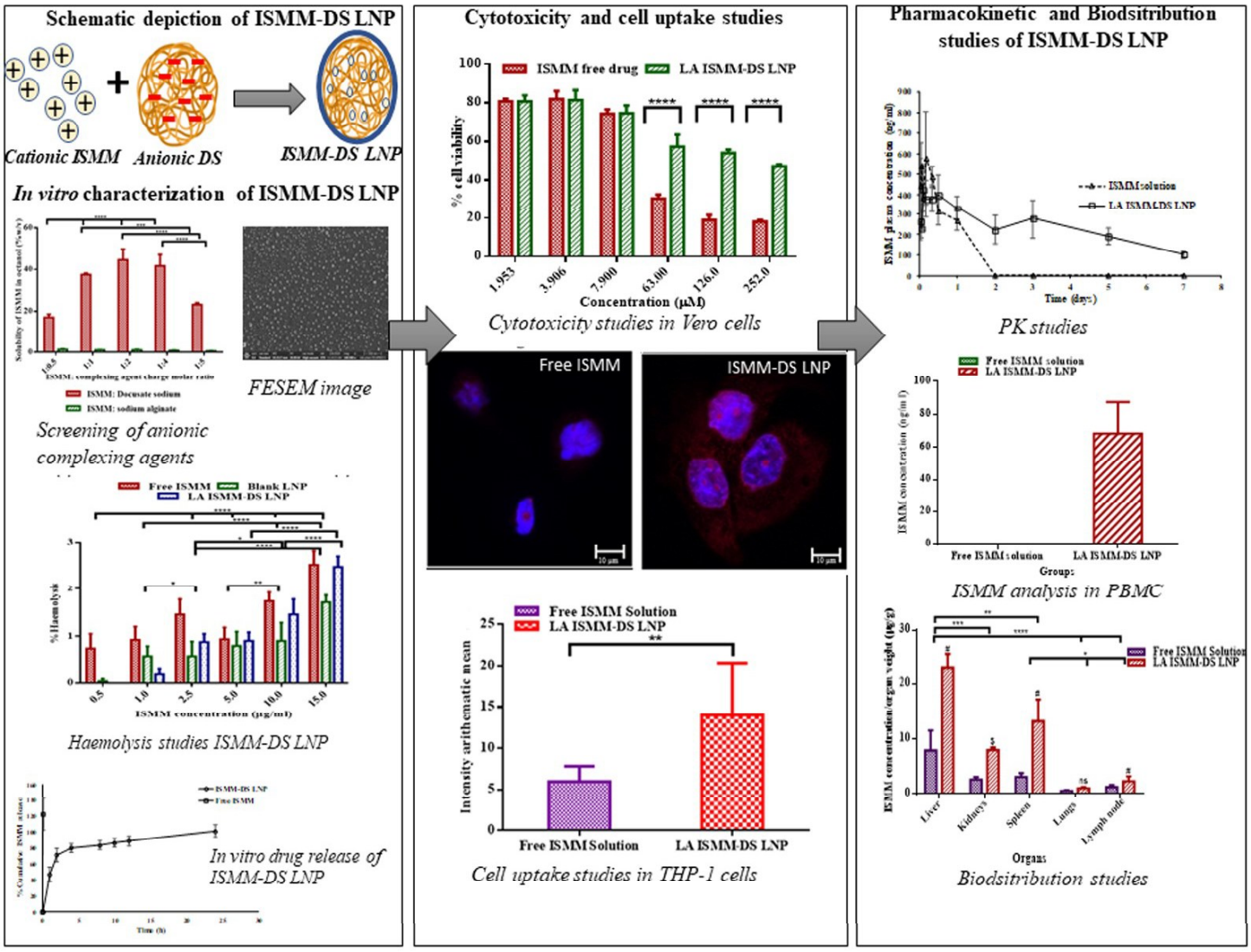

1. Introduction

Isometamidium chloride (ISMM) (M.W. 496 g/mol) [1] is an amphiphilic cationic moiety due to the presence of quaternary nitrogen in phenanthridine ring and hydrophobic phenyl ring in its chemical structure [2]. It is highly water-soluble (6% w/v) with low log P (0.78) and high pKa (11.45). It has half-lives of 0.13, 1.22, and 120.7 h derived by tri-exponential equation upon intravenous administration in cattle [3]. Furthermore, ISMM has the tendency of rapid biodistribution to the liver and kidney causing inefficient plasma concentration below its minimum effective concentration (MEC)(1-4 μg/ml) [4,5]. It is available in the market with various brand names like Samorin®, Trypamidium®, Veridium®, Securidium® [6].

ISMM is used for treatment and prophylaxis of animal African trypanosomiasis (sleeping sickness). Animal African trypanosomiasis is a major cause of concern leading to serious economic deprivation and livestock death in underprivileged rural areas of Africa, America, and Asia [7,8]. It is engendered due to unicellular hemoflagellated protozoan parasites of the genus *Trypanosoma* [6]. Expediency of ISMM amongst other available drugs in the market including diminiazene diaceturate and homidium bromide for treatment and prophylaxis against various trypanosomal strains including *T. evansi, T. congolense, T. vivax and T. brucei* coax to its high market value [9–13]. However, it suffers from drawbacks including inefficient plasma concentration causing frequent relapse and variation in prophylactic effect [14], low efficacy, and high systemic toxicity [15]. Nanocarriers have long been established to decrease toxicity and enhance efficacy. Recently, sodium alginate nanoparticles encapsulating ISMM showed reduced toxicity and low haemolytic potential in horse PBMC and RBC respectively; upon treatment with ISMM-sodium alginate nanoparticles [15]. Similarly, a sustained drug release poly(lactic-co-glycolic)acid cylindrical implants were synthesized for long term ISMM delivery with enhanced efficacy against *T. congolense* by a

factor of 3.2 when implanted subcutaneously in cattle [16]. However, incisional procedures were desirable for the administration of implants. Protracted plasma drug release could be achieved by the development of ISMM nanoformulation; which upon SC/IM administration would lead to primary (injection site) and secondary (immune cell) ISMM depot genesis.

Long-acting lipid nanoparticles have long been explored to achieve protracted plasma drug release for weeks/months due to their biocompatibility and safety profile [17]. The inception of this naïve invention would eliminate lacunae associated with available ISMM marketed formulation and elicit effective treatment and prophylaxis. However, the physicochemical properties of ISMM including log P, water-solubility, pKa was a major defiance for loading ISMM into hydrophobic lipid nanocarriers [2]. Therefore, the present research work was the first manoeuvre to modify the physicochemical properties of ISMM by ionic complexation and suitably encapsulating the formed complex into solid lipid nanoparticles (LA ISMM-DS LNP). The objective involved the development of long-acting (LA) LA ISMM-DS LNP with reduced cytotoxicity, enhanced intracellular delivery and substantial primary and secondary depot to achieve protracted plasma and tissue drug concentration.

2. Materials and methods

2.1 Materials

ISMM was procured from Marvel drugs Ltd. (Mumbai, India), precirol® ATO 5, compritol® 888 ATO, and geleol™ mono and diglyceride NF were kind gift sample from Gattefosse India Pvt. Ltd. (Mumbai, India). Stearic acid, docusate sodium, PEG 2000, dichloromethane, and polyvinylpyrrolidone were purchased from S D Fine-Chem Limited (Mumbai, India), dextran sulphate (M.W. >500,000) and gentamycin (50 mg/ml) was procured from Sigma-Aldrich Chemicals Company (Missouri, United States). dimethyl sulfoxide Cell culture reagent, dulbecco's modified eagle medium (DMEM), Rosewell park memorial institute 1640

(RPMI 1640), glutaraldehyde (25% w/w), dulbecco's phosphate buffer saline (DPBX-10X), and fetal bovine serum were purchased from HiMedia Laboratories Pvt. Ltd. (Mumbai, India). Tween 80, trehalose, 4',6-diamidino-2-phenylindole (DAPI), and thiazolyl blue tetrazolium bromide (MTT) were obtained from Sisco Research Laboratories Pvt. Ltd. (Mumbai, India). Sucrose, n-octanol, ethanol, and Phorbol-12-myristate-13-acetate (PMA) were purchased from Central Drug House (New Delhi, India), Spectrochem Pvt. Ltd (New Delhi, India), Jabsen and Jabsen Co. (GmbH, Germany), and Cayman chemical company respectively. Ficoll-Opaque Plus was procured from GE Healthcare (Chicago, United States). Isopropyl alcohol was obtained from Merck Ltd. (Mumbai, India). THP-1 and Vero cell lines were purchased from National Centre for Cell Science (Pune, India). ultrapurified water was obtained from Milli-Q system (Millipore GmbH, Germany).

2.2. Screening of anionic complexing agents

Docusate sodium (DS), sodium alginate, and dextran sulfate (Mwt: 500000) were screened to prepare ionically complexed ISMM by the modified solubility method [18]. Briefly, a two-phase solvent system was prepared by mixing of 1-octanol and Milli Q in a 1:1 ratio. Thereafter, a known amount of ISMM and anionic complexing agent was added into 2 ml of the above solvent system. The amount of ISMM was kept constant while, the amount of complexing agent was varied to obtain different drug/complexing agent charge molar ratios, including 1:0.5, 1:1, 1:2, 1:4, and 1:5. The Eppendorf were incubated in a water bath shaker (100 rpm, 40°C) for 30 min. The n-octanol phase was diluted using a warm mixture of ethanol/0.3 M calcium chloride and centrifuged at 9000 rpm for 15 min. Whereas, the aqueous phase was diluted using mobile phase and centrifuged at 9000 rpm for 15 min. Both the phases were then analyzed by the developed and validated RP-HPLC method.

2.3.1. Preparation of ISMM-DS complex

ISMM (1 charge molar ratio equivalent) was added to 1 ml of docusate sodium aqueous solution (4 charge molar ratio equivalent) to precipitate ISMM-DS hydrophobic complex. Thereafter, ISMM-DS complex was redispersed in Milli Q water and centrifuged at 9000 rpm for 10 min. The supernatant containing free ISMM and DS was separated from ISMM-DS complex. The complex was freeze-dried and stored at 4°C until further use.

2.3.2. Characterization of ISMM-DS complex

Fourier transform infrared spectroscopy (FTIR)

ISMM, DS and ISMM-DS complex were analyzed by Bruker alpha-one FTIR spectrophotometer (Bruker Optik, Germany) after placing an individual sample (5 mg) on ZnSe sample crystal and scanning the spectra from 3800- 600 cm^{-1}.

2.4 Preparation of ionically-complexed ISMM-docusate sodium complex loaded lipid nanoparticles (LA ISMM-DS LNP)

LA ISMM-DS LNP was prepared by solvent evaporation using *in situ* complexation, as described previously [19]. Briefly, ISMM (10 mg) was dissolved in 10 ml aqueous solution of tween 80 (1% w/v). Docusate sodium (36 mg) and Precirol® ATO 5 (50 mg) were dissolved in dichloromethane (2 ml) to form an organic phase. The organic phase was added to the aqueous phase and homogenized using IKA® T10 basic Ultra Turrax® at 15000 rpm for 5 min to form o/w emulsion. The emulsion was probe sonicated using a probe sonicator (Sonics & Materials, Inc., USA) at 500 watt and 25% amplitude for 150 sec. Thereafter, the organic solvent was evaporated using a rotary evaporator (Buchi rotavapor®, Mumbai, India) at 30°C for 20 min to obtain LA ISMM-DS LNP nano-dispersion which was stored at 4°C until further use.

2.5 Characterization of LA ISMM-DS LNP

2.5.1. Particle size (PS), polydispersity index (PDI) and zeta potential (ʒ-potential)

The aqueous nano-dispersion of LA ISMM-DS LNP obtained in section 2.4 was centrifuged at 48000 rpm at 4ºC for 20 min using Sorvall™ Ultracentrifuge (Thermo Scientific, Waltham, United States). The pellet obtained after ultracentrifugation was redispersed and diluted using Milli Q water. PS, PDI, and ʒ-potential of diluted samples were measured by photon correlation spectroscopy using Malvern Nano ZS (Malverns instrument Ltd., UK) at 30ºC.

2.5.2. % entrapment efficiency (%EE)

The supernatant obtained after centrifugation as described above was diluted with the mobile phase and analyzed using validated RP-HPLC method for ISMM. % EE was further determined using equation (5.1)

$$\%\ \text{entrapment efficiency} = \frac{\text{Total amount of drug added} - \text{amount of drug in supernatant}}{\text{Total amount of drug added}} \times 100 \ldots . (5.1)$$

2.5.3 Field-emission Scanning Electron Microscopy (FESEM)

The redispersed pellet as obtained in section 2.5.1 was diluted 50 times in Milli Q and a drop was applied on glass coverslip. The sample applied on glass coverslip was dried overnight at room temperature and the coverslip was attached to a metal stub by two-way carbon tape. The sample was gold-coated for 120 s using Quorum Technologies Q150TES sputter coater (East Sussex, England). Gold-coated nanoparticles were then analyzed by FEI™ scanning electron microscope (Hilsboro, Washington) at 20KV high vacuum, 100000X magnification with a spot size of 9.0, and a scale of 500 nm.

2.6 Lyophilization of LA ISMM-DS LNP

2.6.1. Screening of cryoprotectants

Various cryoprotectants, including trehalose, sucrose, PEG 2000, and PVP were screened for lyophilization of LA ISMM-DS LNP. Briefly, pellets obtained after ultracentrifugation of LA ISMM-DS LNP were redispersed in an aqueous solution (20%w/v) of the above-stated cryoprotectant and freeze-dried using benchtop FreeZone Triad Free Dry system (Labconco, USA) with pre-freezing at -80°C for 12 h followed by vacuum drying for 24 h.

2.6.2 Optimization of the lyophilization cycle

LA ISMM-DS LNP pellets obtained after ultracentrifugation as described above (section 2.5.1) were redispersed in trehalose aqueous solution (20% w/v) and pre-frozen at -80°C for 12 h, vacuum dried from -50°C to 4°C for 19 h; thereafter, the temperature was slowly raised to 20°C in 7 h to evaporate traces of moisture. The ramp was kept constant at 0.25°C. The lyophilized LA ISMM-DS LNP was dispersed in Milli Q water (50 mg/ml) to determine PS, PDI, ʒ-potential as described in section 2.5.1. Further, LA ISMM-DS LNP (10 mg) was added in 1 ml of water: methanol (50:50 %v/v) and bath sonicated for 15 min. Aliquote of bath sonicated ISMM-DS LNP solution was then diluted in the mobile phase and analyzed by validated RP-HPLC method for estimation of ISMM after centrifugation (15000 rpm, 10 min) using Eppendorf, 5430 R centrifuge as described in chapter 3.

2.7 *In vitro* drug release studies

In vitro drug release studies were carried out by adding LA ISMM-DS LNP into 50 ml 0.2% sodium lauryl sulphate solution maintained at 37°C at 200 rpm. An aliquot (3 ml) was withdrawn at 1, 2, 4, 8, 10, 12, and 24 h and centrifuged using Sorvall^{TM} Ultracentrifuge (Thermo Scientific, Waltham, United States) at 48000 rpm for 20 min at every time point.

The supernatant was collected, and the pellet was redispersed in release media and added back to the dissolution medium.

2.8 Blood compatibility studies

Haemolysis assay was performed to confirm the blood compatibility of LA ISMM-DS LNP as described previously with some modification [20]. Briefly, 500 µl of blood was obtained from male Wistar rats and centrifuged using REMI cooling centrifuge at 1000 rpm for 5 min to yield RBC pellet. The pellets were washed with 250 µL normal saline and again separated by centrifugation, after which the RBCs were diluted in a 4:1 ratio with normal saline. Obtained RBC suspension 50 µL each was treated with 50 µL of 0.5, 1, 2.5, 5, 10 and 15 µg/ml free ISMM, ISMM equivalent of LA ISMM-DS LNP or Blank LNP by incubation at 37°C for 30 min. Milli Q water and normal saline was used as control. Thereafter, normal saline was added upto 1 ml, and the sample centrifuge tube was centrifuged at 1000 rpm using REMI cooling centrifuge for 5 min. The optical density of 100 µl of supernatant was determined by Epoch Elisa plate reader (BioTek U.S., Winooskii) at 540 nm to yield % hemolysis using equation 5.2

$$Haemolysis\ (\%) = \frac{\text{ODsample} - \text{ODnegative control}}{\text{OD positive control} - \text{ODnegative control}} * 100 \ldots . (5.2)$$

The treated RBC pellet (50 µl) was diluted 20 times with normal saline. Thereafter, 100 µl of the suspension was fixed with 100 µl glutaraldehyde solution (2.5% in normal saline). Aliquote (50 µl) of the above suspension was placed on a coverslip and dried overnight at 4°C. The fixed cells were treated with normal saline and dehydrated with ethanol serially using 50% w/v and 100% w/v ethanol and allowed to dry at 37°C for 1 h. Thereafter, the coverslip were fixed on glass slides and observed under Carl ZEISS Axio microscope (Jena, Germany) and images were processed using ZEN 2.3 lite software [21].

2.9 *In vitro* cytotoxicity and cell uptake studies

2.9.1 Cells

Adherent Vero cells were cultured in DMEM media containing 10% FBS in a T-75 culture flask incubated in humidified 37℃, 5% CO_2 incubator for 15 days until the flask becomes confluent. Whereas, THP-1 suspension cells were suspended in RPMI-1640 media enriched with 10% FBS in a T-75 culture flask and incubated in humidified 37℃, 5% CO_2 for 6 days to obtain optimal cell count ($11*10^6$ cells/ml).

2.9.2 *In vitro* cytotoxicity studies in Vero cells

In vitro cytotoxicity studies were carried on Vero cells. Briefly, 7000 cells/well in complete DMEM were seeded in 96 well plates 12 h prior and incubated at 37 °C with 5% CO_2. Free ISMM and LA ISMM DS LNP were diluted in DMEM media enriched with 10% FBS to obtain 1.9, 3.9, 7.9, 63.0, 126.0, and 252.0 µM of ISMM. The media was removed, and cells were treated for 24 h at 37°C and 5% CO_2 with 100 µl of different concentrations of prepared free ISMM solution or LA ISMM-DS LNP dispersion. Thereafter, supernatant was removed after treatment, and cells were treated with 100 µL of MTT reagent (500µg/ml) for 4h in a humidified 37°C,5% CO_2 incubator. The reagent was then removed and formazan crystal dissolved in 100 µl of DMSO. The absorbance was then obtained using Epoch Elisa plate reader (BioTek U.S., Winooskii) at 570 nm, which was used to calculate % cell viability (equation 5.3).

$$\%\ cell\ viability = \frac{\text{abs sample} - abs\ blank}{abs\ control - abs\ blank} * 100 \ldots\ldots\ldots (5.3)$$

2.9.3 Cell uptake studies

THP-1 macrophage-like cells ($5*10^4$ cells) were suspended in complete RPMI 1640 media containing PMA (0.1 ng/ml) on a coverslip in each well of 6-well plate for 48 h in CO_2 incubator (37°C and 5% CO_2). Thereafter, the supernatant was removed and cells were incubated with free ISMM or LA ISMM-DS LNP suitably diluted in RPMI 1640 complete media to yield 6.0484 µM ISMM equivalent at 37°C for 1 h and 5% CO_2. Further, the supernatant was removed and cells were washed with DPBS (1X) thrice. The cells were fixed with glutaraldehyde (2.5% in DPBS) and counterstained with DAPI (1µg/ml) for 15 min in dark. The cells were again washed using DPBS (1X) and coverslip fixed on a glass slide and observed under Carl ZEISS Axio fluorescent microscope with apotome attachment (Jena, Germany) at 63X and fluorescence intensity of the images was obtained by deriving histogram of each image using ZEN 2.3 software.

2.10 *In vivo* pharmacokinetics and biodistribution studies of LA ISMM-DS LNP

In vivo pharmacokinetics and biodistribution study protocols were approved by the Institutional Animal Ethics Committee of Birla Institute of Technology and Science, Pilani campus, Pilani (Protocol no.: IAEC/RES/22/03/Rev-1/24/19). Adult male Wistar rats (285.0±50.0 g) were acclimatized for a week on a regular 12 h light-dark cycle, housed in a well ventilated cage with access to food and water *ad libitum*. The animals were divided into two groups (n=4). Free ISMM (30 mg/kg) and LA ISMM-DS LNP (30 mg/kg ISMM equivalent) were subcutaneously injected in flank tissue in group I and II respectively. For pharmacokinetic study, 300 µl of blood was withdrawn at 0, 0.020, 0.042, 0.083, 0.160, 0.33, 0.5,1, 2, 3, 5 and 7 days in heparinized tubes from retro-orbital plexus. Plasma was separated from the blood after centrifugation at 7500 rpm for 10 min using REMI cooling centrifuge and stored at -80°C until further use. The animals were anesthetized at the 7^{th} day followed by cervical dislocation to obtain organs including liver, spleen, kidneys, lungs, brain, and

lymph node to determine drug content. The organ samples were suitably washed with normal saline, excess of liquid was absorbed onto an absorbent paper and stored at -80°C until further use. ISMM was extracted from biological matrices and analyzed by RP-HPLC as described previously (section 2.3.4 and 2.3.5; chapter 3). Upon determination of ISMM concentration in plasma at each time-point, the pharmacokinetic profile was obtained. The pharmacokinetic parameters were calculated by non-compartmental analysis using WiNonlin software. While, drug concentration per gram organ weight was determined after extraction of ISMM from each organ to estimate the biodistribution profile of free ISMM and LA ISMM-DS LNP.

2.11 Statistical analysis

Data of all *in vitro* studies were represented as mean±SD with 3 biological replicates, while *in vivo* experiments were represented as mean±SEM with 4 biological replicates to obtain statistically significant results. The results obtained were analyzed using Graphpad prism 6.01. Specific comparisons between two groups were performed using a student t-test with $p<0.05$ as a minimal level of significance. Mathematical fit functions were performed by ANOVA analysis.

3. Results and Discussion

3.1.1 Screening of anionic complexing agents

Hydrophobic ionic complexation has been recently evolved to amend the solubility of small and large charged hydrophilic molecules. Majorly, carboxylic acid salts, and sulfate-containing molecules have been used for the formation of hydrophobic ionic complex (HIC) with decreased water solubility [22–24]. Therefore, sodium alginate (sodium salt of D-galactouronic acid), dextran sulphate, and docusate sodium (dioctyl sodium sulfosuccinate) (DS) were screened as anionic complexing agents to form HIC.

When the solubility of free ISMM was determined in the aqueous phase, the amount of free ISMM decreased upon an increase in charge molar ratio of ISMM: DS and ISMM: sodium alginate depicting ISMM HIC formation. Furthermore, the concentration of free ISMM in aqueous phase was higher when complexed with docusate sodium in comparison with sodium alginate. This could be due to insoluble suspended particles observed in the aqueous phase which were centrifuged and separated before analysis leading to erroneous observation. However, an increase in charge molar ratio of ISMM: dextran caused no significant difference in solubility of free ISMM in the aqueous phase. The solubility of free ISMM in water was higher when complexed with dextran sulphate (M. W. 500000) in comparison to ISMM:DS and ISMM: sodium alginate (Figure 5.1(a)).

Since dextran sulphate failed to elicit efficient complexation of ISMM; therefore, the solubility of the ISMM complex in 1-octanol was determined for various charge molar ratios of ISMM:DS and ISMM: sodium alginate. Maximal complexation must occur at a 1:1 charge molar ratio of anionic complexing agent and ISMM. However, increased shielding or steric hindrance of the complexing agent leads to poor complexation due to low exposure of charged group at 1 charge molar ratio of ISMM and anionic complexing agent. Similar observations were reported earlier when verapamil was ionically complexed with dextran sulphate and loaded into solid lipid nanoparticles. Maximal complexation and entrapment of verapamil occurred at a higher charge molar ratio (>1) of anionic complexing agent and ISMM [22]. An increase in charge molar ratio of DS or sodium alginate led to an increase in the formation of ISMM HIC (Figure 5.1(b)).

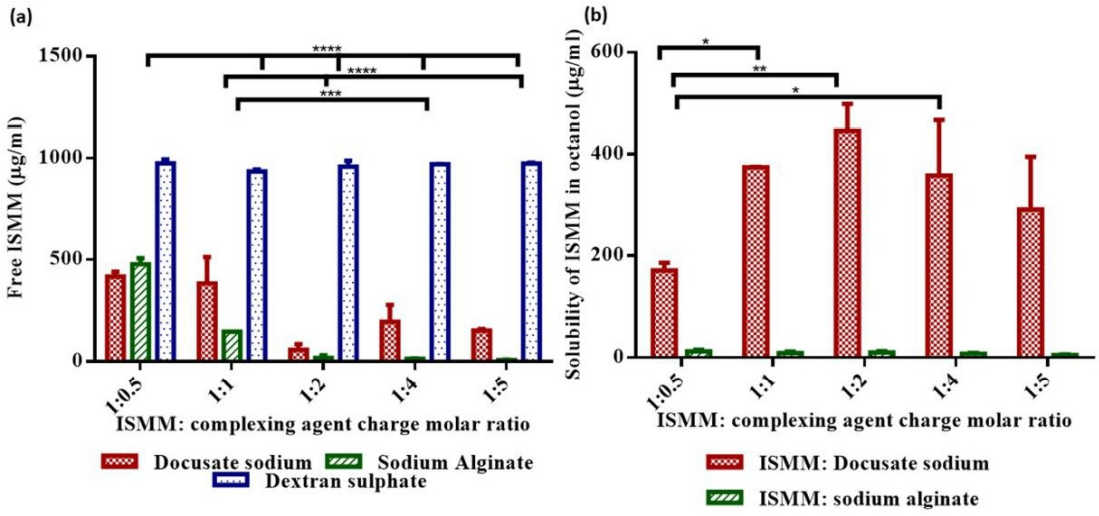

Figure 5.1 Screening of anionic complexing agent (a) Solubility of free ISMM in water upon complexation with docusate sodium, sodium alginate or dextran sulphate at various charge molar ratios. (b) Solubility of hydrophobic anionic complex in n-octanol upon complexation with docusate sodium or sodium alginate at charge molar ratio of 1:0.5 to 1:5. Data represents mean±SD, n=3 * represents $p<0.05$ and ** represents $p<0.01$, *** represents $p<0.001$, **** represents $p<0.0001$ for two-way ANOVA followed by Tukey's multiple comparison test.

The solubility of ISMM-DS complex in n-octanol increased from 170.6±15.29 µg/ml to 358.3±108.41 µg/ml when the charge molar ratio of ISMM and DS was increased from 1:0.5 to 1:4. Micelle formation would occur upon further increase in anionic complexing agent causing solubilization of ISMM-DS LNP; thereby decreasing its n-octanol solubility. Whereas, the solubility of ISMM HIC when complexed with sodium alginate was less in comparison with DS and was found to decrease from 12.6±3.07 µg/ml to 8.3±1.30 µg/ml at 1:0.5 to 1:4 charge molar ratio of ISMM: sodium alginate. The log P of DS, sodium alginate, and dextran sulphate is 5.24, -2.6, and -7.2, respectively [25–27]. Therefore, the complexation ability of the three anionic complexing agents was found to be in the order of DS>sodium alginate> dextran sulphate which owing to log P of individual complexing agent.

Anionic complexing agents tune the solubility of charged hydrophilic moiety via two-step mechanism wherein; initially the complexing agent disguises the charge of the hydrophilic molecule by ion-pairing diminishing its solubility in water. Later, the hydrophobic group of

complexing agents including alkyl or aromatic group inlay over the surface of hydrophilic moiety and further decrease its water solubility [28]. A decrease in HIC formation with dextran sulphate could be attributed to its decreased charge/surface area ratio owing to its higher molecular weight (MW>500,000). While docusate sodium encompasses higher hydrophobicity due to the alkyl side chain in comparison to sodium alginate causing reduced n-octanol solubility of sodium alginate-ISMM HIC.

3.1.2. Characterization of ISMM-DS complex

Fourier transform infrared spectroscopy (FTIR)

The ISMM-DS HIC was evaluated by FTIR spectroscopy at ISMM: DS charge molar ratio of 1:4. DS forms an ionic complex with quaternary nitrogen present in phenanthridine ring of ISMM. Upon complexation of ISMM with DS the aromatic C-N stretch (1389-1260 cm^{-1}) of the quaternerized nitrogen in ISMM (Figure 5.2) disappeared as evidenced by FTIR spectra of ISMM-DS complex. Furthermore, the N=N- stretch of ISMM was shifted from 1460 cm^{-1} to 1452 cm^{-1} in ISMM-DS complex. While the aromatic C-H stretch of meta-position for ISMM was shifted from 700 cm^{-1} to 651 cm^{-1} but, the N-H stretch (3851cm^{-1} to 3563cm^{-1}) of ISMM was intact in IR spectra of LA ISMM-DS LNP. Peak at 2934 cm^{-1} and 2858 cm^{-1} corresponds to -CH and -CH_2 stretching, while the peak at 1730 cm^{-1} corresponds to C=O stretch depicting the presence of docusate sodium. Further, a peak at 1384 cm^{-1} was prevalent in ISMM-DS complex as well as docusate sodium revealing the presence of sulfate group. Therefore, FTIR spectroscopy confirmed the complexation of ISMM with DS.

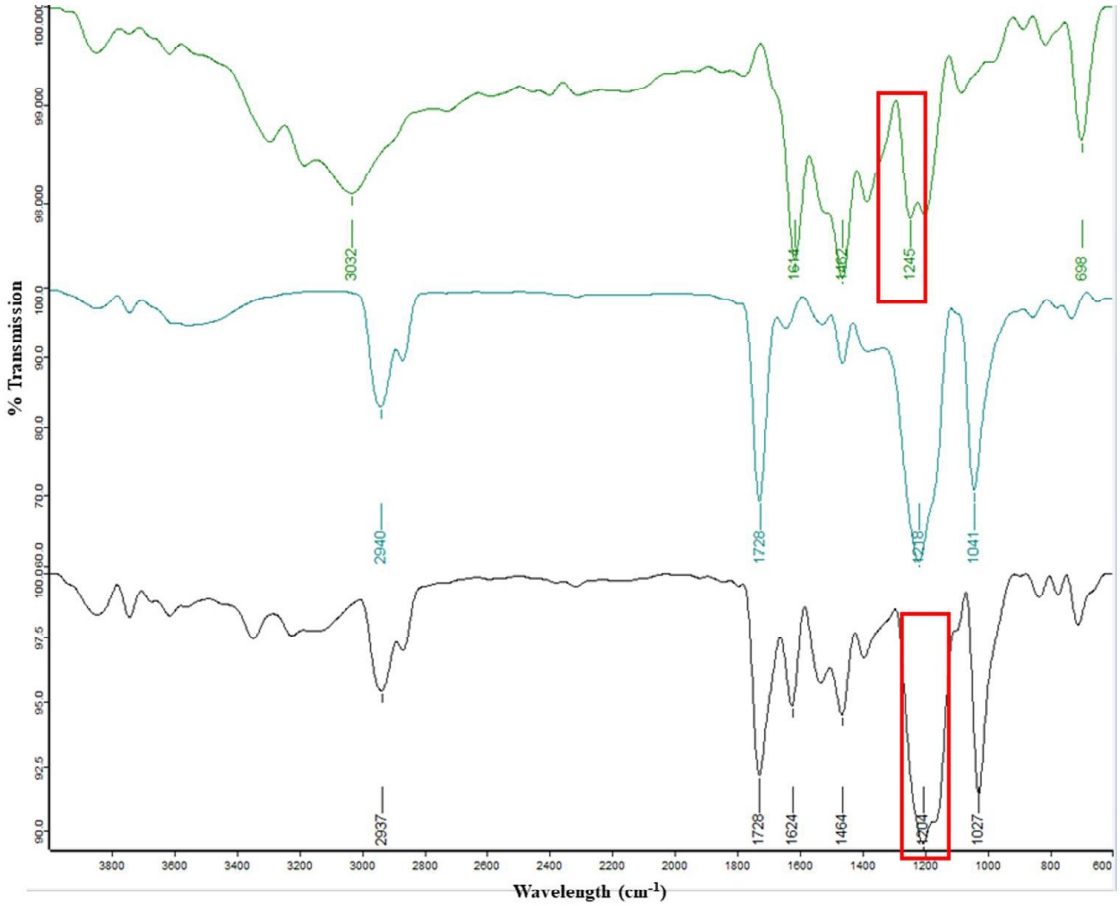

Figure 5.2 *In vitro* characterization of ISMM-DS complex depicting FTIR spectra of ISMM, DS and ISMM-DS LNP from top to bottom.

3.2 Preparation and characterization of LA ionically complexed LA ISMM-DS LNP

A preliminary synthesis of ISMM-LNP was initiated solely by the solvent evaporation method resulting in poor % EE (Table 5.1). Therefore, further development of LA ISMM-DS LNP were done by novel *in-situ* complexation followed by the solvent evaporation technique. The optimization of LA ISMM-DS LNP were done by risk-based approach wherein critical process parameters (CPP) and critical formulation parameters were identified as depicted in Ishikawa diagram (Figure 5.3) which would affect the Quality target product profile (QTPP) including PS, PDI and %EE of LA ISMM-DS LNP. The effect of process parameters which include homogenization speed and time, sonication energy, and sonication time and rate of organic solvent evaporation has been well established [29,30]. Therefore,

critical formulation parameters were a prominent cornerstone for the development of LA ISMM-DS LNP. Non-ionic surfactant (tween-80-1% w/v) was utilized for the development of LA ISMM-DS LNP to avoid destabilization of formed ISMM-DS ionic complex upon utilization of anionic/cationic surfactants. Furthermore, tween-80 have long been considered for parenteral administration owing to its GRAS status [31].

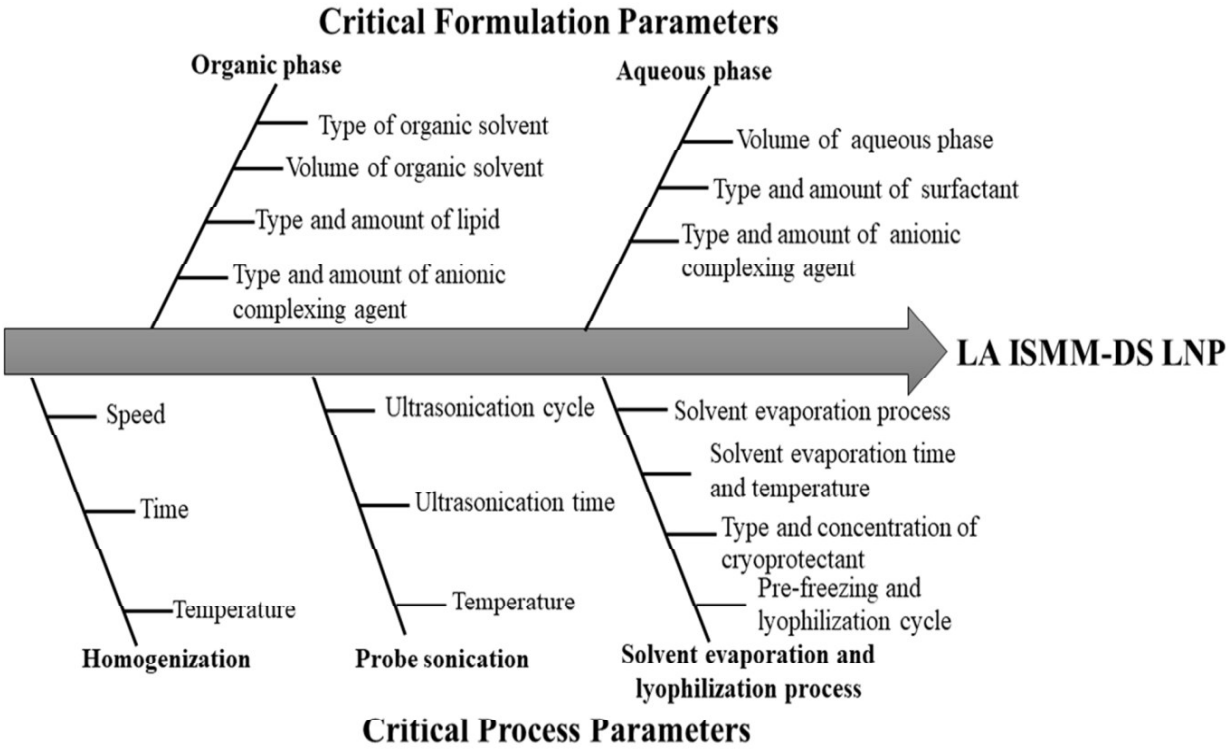

Figure 5.3 Ishikawa diagram predicting critical formulation and process parameters for LA ISMM-DS LNP.

Table 5.1 Formulation development and optimization of LA ISMM-DS LNP by risk-based approach

Batch code	**Ingredients**						**Particle size ±SD (n=3)**	**PDI ±SD (n=3)**	**Zeta potential ±SD (n=3)**	**% EE±SD (n=3)**
	Lipids (mg)				Complexing agents (mg)					
	Precirol	Compritol	GMS	Stearic acid	Dextran Sulphate	DS				
ISMM-Prec LNP: Formulation variable; amount of lipid										
ISMM-Prec01	10	-	-	-	-	-	249.7 ± 18.13	0.54 ± 0.14	-9.3 ± 1.27	1.1 ± 0.17
ISMM-Prec02	50	-	-	-	-	-	241.2 ± 29.96	0.34 ± 0.04	-10.6 ± 0.36	1.6 ± 0.11
ISMM-Prec03	100	-	-	-	-	-	276.9 ± 23.74	0.49 ± 0.18	-9.0 ± 1.63	3.6 ± 0.21
ISMM-Com: Formulation variable; Type of complexing agent										
ISMM-Com01	50	-	-	-	20	-	266.1 ± 28.05	0.28 ± 0.04	-36.3 ± 9.45	18.2 ± 1.60
ISMM-Com02	50	-	-	-	-	18	286.3 ± 23.42	0.32 ± 0.03	-27.4 ± 4.17	64.9 ± 2.55
ISMM-DS LNP: Formulation variable; lipid screening										
ISMM-DS01	50	-	-	-	-		286.3 ± 23.42	0.32 ± 0.03	-27.4 ± 4.17	64.9 ± 2.55
ISMM-DS02	-	50	-	-	-	18	599.0 ± 25.94	0.33 ± 0.04	-25.5 ± 3.31	63.2 ± 3.56
ISMM-DS03	-	-	50	-	-	18	998.7 ± 29.51	0.61 ± 0.05	-28.2 ± 2.52	62.1 ± 4.12
ISMM-DS04	-	-	-	50	-	18	352.1 ± 19.13	0.30 ± 0.05	-39.7 ± 5.02	47.2 ± 1.28
ISMM-DS LNP: Formulation variable; Amount of DS										
ISMM-DS01	50	-	-	-	-	27	215.50 ± 6.30	0.26 ± 0.03	-41.3 ± 3.01	64.26 ± 1.12
ISMM-DS02	50	-	-	-	-	36	173.17 ± 10.70	0.22 ± 0.02	-48.3 ± 2.02	69.14 ± 1.27

All formulation contained 10 mg ISMM and tween 80 (1% w/v) in 10 ml aqueous phase, DS: Docusate sodium

Type and amount of lipid

Various lipids including precirol® ATO 5 (glyceryl palmitostearate), compritol® 888 ATO (glyceryl dibehenate) and geleol™ mono and diglyceride NF (glyceryl monostearate) and stearic acid were screened for preparation of LA ISMM-DS LNP. Precirol® ATO 5 although contains a fatty acid chain yet it terminates with hydrophilic hydroxyl groups yielding a favourable environment for solubilization and nanoprecipitation of LA ISMM-DS LNP [32]. However, compritol® 888 ATO consists of triglycerides which enhance the hydrophobicity causing increased encapsulation of LA ISMM-DS LNP. However, the interfacial tension would be drastically increased during solvent evaporation using dichloromethane leading to an increase in particle size. Furthermore, an increase in polymorphic transition of compritol® 888 ATO could have also led to increased particle size [33,34]. A similar observation was reported for geleol™ mono and diglyceride NF wherein; the formed nanoparticles quickly aggregated upon solvent evaporation due to the orderly arrangement of lipid crystals in glyceryl monostearate in comparison to precirol® ATO 5 and compritol® 888 ATO causing inefficient surface area for surfactant stabilization [35]. Furthermore, hydrophobic character and crystalline nature with miniscule space for incorporation of ISMM-DS HIC could have led to decreased encapsulation and slight increase in particles size when stearic acid was used as lipid carrier. Although, increase in amount of lipid impeled increase in %EE; however, it was associated with undesirable increase in particle size and PDI.

Type and level of anionic complexing agent

Dextran sulfate and DS were screened as anionic complexing agents for the development of LA ISMM-DS LNP. The results corroborated with the preliminary screening of anionic complexing agents wherein; lower encapsulation efficiency was obtained with dextran sulfate. The molecular weight, log P, and polar surface area are indispensable factors for HIC formation [28]. The lower complexation potential of dextran sulphate could be attributed to

its higher molecular weight and lower charge/surface area ratio compared with docusate sodium. Furthermore, 1.24-folds decrease in particle size accomplished with 1:4 charge molar ratio of ISMM:DS could be due to enhanced stearic stabilization obtained with increased docusate sodium in LA ISMM-DS LNP. The optimized LA ISMM-DS LNP using precirol® ATO 5, DS, and tween 80 as lipid, anionic complexing agent, and surfactant led to nanoparticles with spherical morphology as evidenced by FESEM analysis (Figure 5.4(a)).

3.3 Lyophilization studies

Synthesis of nanoparticles involves the application of energy during homogenization or probe sonication piqued with an increase in Gibb's surface free energy of nanoparticles which is compensated by the stabilizer. Conversion of aqueous nanoformulation into solid-state by lyophilization is a pre-requisite for long-term storage stability. However, the steric stabilization elucidated by surfactants/stabilizers become ineffective during freezing causing irreversible aggregation and loss of effective redispersibility after lyophilization [36]. Furthermore, crystallization of water will still enhance the mechanical destabilization of nanoparticles. The incorporation of nanoparticles into a glassy state will prevent the destabilization of nanoparticles. Thus, arousing the demand for cryoprotectants [37]. Various cryoprotectants including PEG 2000, PVP, sucrose, and trehalose were screened in 20% w/v concentration to prevent the aggregation of the nanoparticles due to mechanical stresses during the freezing and lyophilization process (Table 5.2). The ability of screened cryoprotectants to elicit cryoprotection of LA ISMM-DS LNP was in the order of trehalose>sucrose>PVP>PEG as determined by their final to initial particle size ratio (S_f: S_i ratio) (Table 5.2). Increased stabilization of LNP obtained with sugars (trehalose and sucrose) due to their enhanced hydrogen bonding competence in comparison with PVP and PEG. Furthermore, carbohydrates decrease the osmotic pressure of crystallizing water, vitrify and provide amorphous glass phase maintaining nanoparticles in static conditions [38]. Amongst

the carbohydrates, LA ISMM-DS LNP depicted enhanced stability when lyophilized using trehalose (S_f:S_i:0.97±0.028; ʒ-potential: -28.6±0.84) (Figure 5.4(b)) in comparison with sucrose (S_f:S_i; 1.84±0.109; ʒ-potential:-12.8±0.77). Lyophilized LA ISMM-DS LNP appeared amorphous bulky powder, with PS, PDI, and drug content of 325.4±37.03 nm, 0.341±0.03 and 4.2±1.36 µg/mg respectively. Further, the lyophilization cycle was optimized to obtain quick redispersibility, S_f:S_i<1.3.

Table 5.2 Screening of cryoprotectants for lyophilization of LA ISMM-DS LNP

Cryoprotectant (20% w/v)	**S_f/S_i**	**I_f/I_i**	**ʒ- potential (mV)**
Trehlose	0.97±0.028	0.83±0.180	-28.6±0.84
PEG	2.13±1.007	1.64±0.488	-21.65±0.63
PVP	1.91±0.432	1.12±0.041	10.65±0.9
Sucrose	1.84±0.109	2.30±0.091	-12.85±0.77

Data represented as mean±SD, n=3

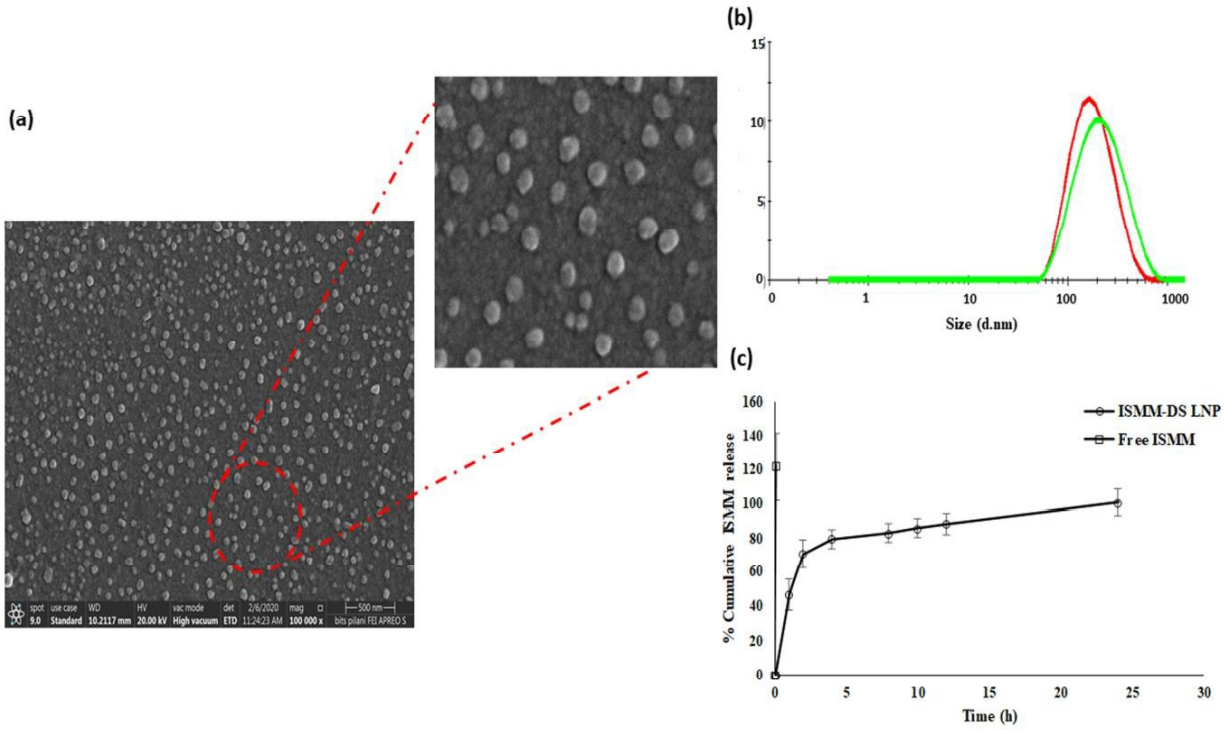

Figure 5.4 *In vitro* characterisation of LA ISMM-DS LNP (a) FESEM image of LA ISMM-DS LNP (b) Particle size distribution of LA ISMM-DS LNP before (red) and after lyophilization (green) (c) *In vitro* drug release studies of LA ISMM-DS LNP (Data represented as mean±SD).

3.4 *In vitro* drug release studies

Efficient ISMM blood and tissue concentration would emanate from the ability of LA ISMM-DS LNP to sustain the drug release of ISMM. The long-term drug release potential of LA ISMM-DS LNP was elucidated under sink condition using sodium lauryl sulphate solution (0.2% w/v) at pH 7.4 to mimic the microenvironment of systemic circulation. The drug release profile depicted 46.3±8.9% ISMM release within 1 h; thereafter, caused sustained drug release leading to plateau until 24 h (Figure 5.4(c)). As per previous reports, the minimum effective concentration (MEC) required to curb parasite load was found to be 1-4 µg/ml [5]. ISMM drug release profile could maintain the desired concentration at every time-point. The initial burst release could be attributed to the anionic characteristic of sodium lauryl sulphate leading to quick ion exchange with DS in the ISMM-DS complex. Similar reports have been established wherein; the release kinetics of hydrophilic tenofovir and emtricitabine when encapsulated into PLGA nanoparticles revealed burst release (~73%) within 22.6 min and 15 min at pH 5.5 which emerged as the driving force for burst release [39]. Additionally, nanosuspension of hydrophilic tenofovir along with lopinavir and ritonavir led to burst release of tenofovir (90%) at 1h upon subcutaneous administration causing lymphatic uptake of meagrely 10% tenofovir [40]. Therefore, it is hypothesized that the subcutaneous administration of LA ISMM-DS LNP may lead to the transfer of drug depot from the primary injection site to immune cells carried through lymphatic vessels drained into the systemic circulation. Whereby; exposure to a larger amount of fluid shall cause drug release within 24 h as evidenced during *in vitro* drug release studies.

3.5 Blood compatibility studies

LA nanoformulations were established for weeks/months-long drug delivery in blood with conjecture of drug-induced haemolysis. Furthermore, trypanosomal infection manifest haemolysis due to flickering flagella and microtubule-reinforced bodies [41]. Moreover, ISMM (> 1 mg/ml) may lead to enkephalocyte formation and haemolysis by osmotic fragility [42]. Therefore, haemolytic potential of developed LA LA ISMM-DS LNP was evaluated in comparison with free ISMM. The % haemolysis was found to be <2.52% for 1.00-30.24 µM ISMM concentration (Figure 5.5(a)-(b)). Moreover, no significant difference was observed in % haemolysis of LA ISMM-DS LNP in comparison with free ISMM depicting blood compatibility of developed LNP.

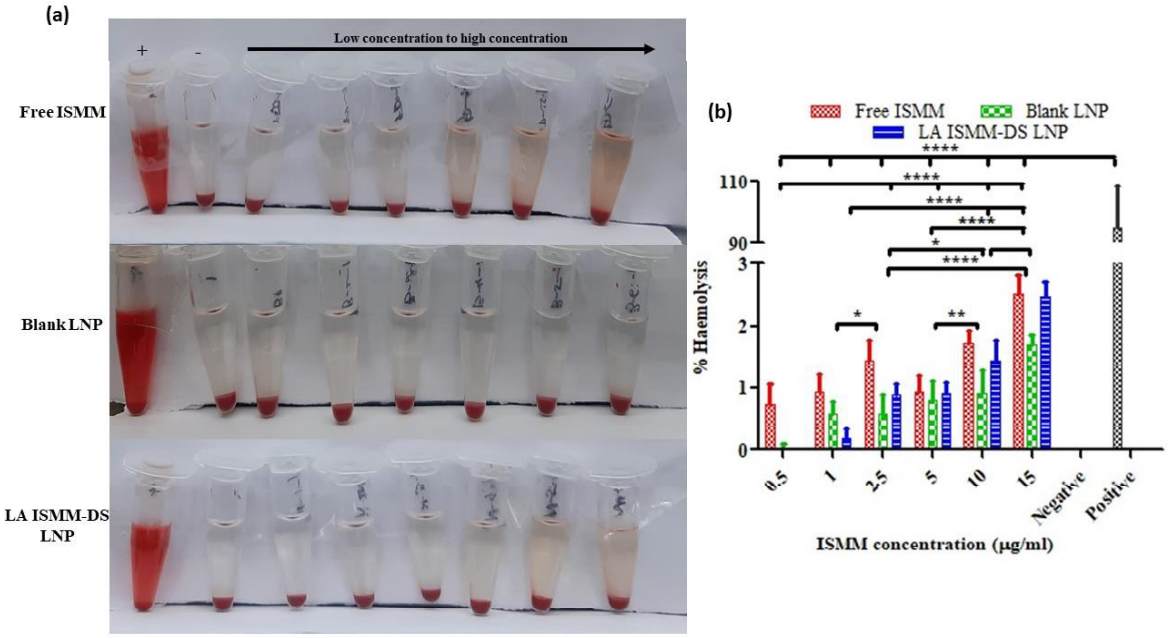

Figure 5.5 *In vitro* blood compatibility studies of LA ISMM-DS LNP (a) Pictorial representation of haemolysis immediately after treatment with free ISMM, blank, and LA ISMM-DS LNP. (b) % haemolysis of free ISMM, blank, and LA ISMM-DS LNP.

Furthermore, the RBC pellet observed after haemolysis study revealed haemolysed irregular RBC in the positive control group. However, the morphology of treated RBC remained intact similar to negative control in free ISMM and LA ISMM-DS LNP treated group (Figure 5.6).

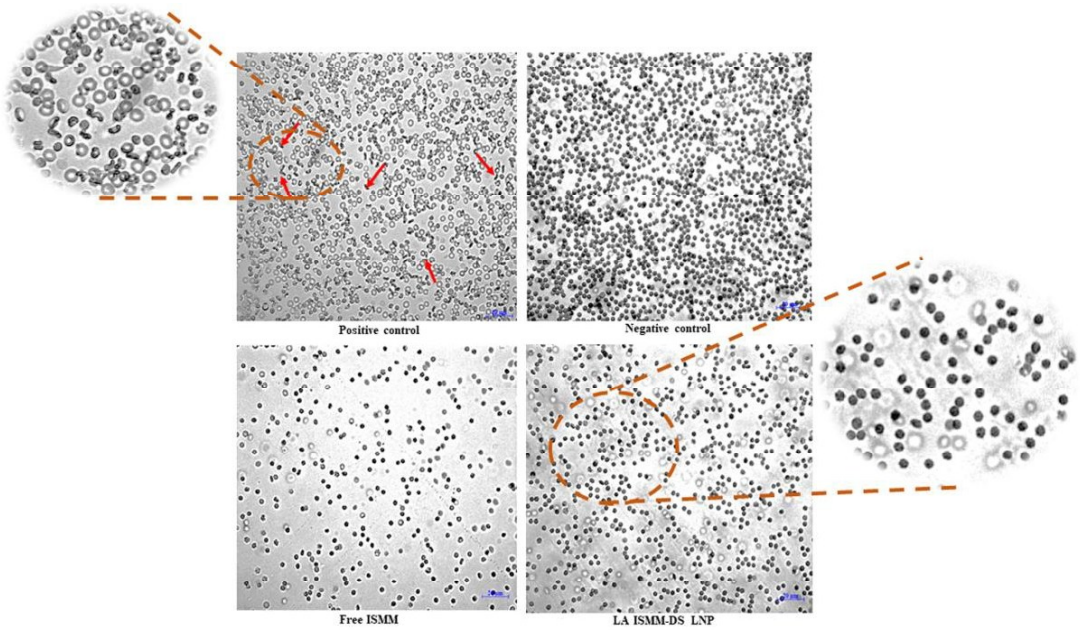

Figure 5.6 Optical micrographs of RBC treated with distilled water (positive control), normal saline (negative control), free ISMM and LA ISMM-DS LNP, respectively.

3.6 *In vitro* cytotoxicity and cell uptake studies

Expeditious disposition of hydrophilic and cationic ISMM into the liver, kidney, and spleen for a prolong period suggests the involvement of specialized membrane transporter for ISMM absorption [2,4]. Organic cationic transporters (OCT) are a class of solute carrier proteins belonging to the 22A gene. It is subdivided into 3 categories including OCT1, OCT2, and OCT3. OCT1 and OCT2 are expressed in liver and kidney proximal tubule respectively. While, OCT 3 receptors are expressed in heart, liver, and skeletal muscles. Many endogenous cationic molecules as well as cationic drugs that cannot cross the lipophilic cellular membrane utilize OCT for their transport. Their role mainly involves detoxification of endogenous cations and drug disposition [43,44]. Vero cells are derived from the kidneys of African green monkey (*Cercopithecus aethiops*) [45] which also express OCT. Therefore, the cytotoxicity studies of LA ISMM-DS LNP were carried on Vero cells. As per the previous

report, the minimum effective concentration (MEC) of ISMM was found to be 2.01-8.06 µM [5]. However, the % cell viability was found to be 74.2±2.29% and 74.6±3.87% at MEC upon treatment with free ISMM and LA ISMM-DS LNP equivalent to ISMM, respectively (Figure 5.7(a)). Upon an increase in ISMM concentration beyond MEC; cell viability was significantly reduced in cells treated with free ISMM solution compared with LA ISMM-DS LNP ($p<0.0001$). To conclude, LA ISMM-DS LNP were cytocompatible compared with free ISMM.

Immune cell (macrophage and T-lymphocytes) infiltration at injection sites cause major impetus for secondary depot genesis of LA nanoformulation injectables [46,47]. Therefore, cellular uptake studies were carried in THP-1 macrophage-like cells and analyzed by inverted fluorescent microscopy with apotome attachment (Figure 5.7(b)). It was observed that the inherent fluorescence of ISMM was 2.3-folds higher when treated with LA ISMM-DS LNP compared with free ISMM ($p<0.05$) (Figure 5.7(c)). Differentiated THP-1 cells elicit higher expression of solute carrier group of membrane transporters including organic cation transporters compared with monocytic THP-1 which are susceptible to carrier saturation [48]. Therefore, uptake of free ISMM would have occurred through membrane transporters, and the results corroborated with established mechanics of THP-1 cellular uptake. However, enhanced uptake of LA ISMM-DS LNP could be attributed to the highly hydrophobic characteristic of lipid carriers along with ISMM-DS HIC leading to their phagocytosis [49].

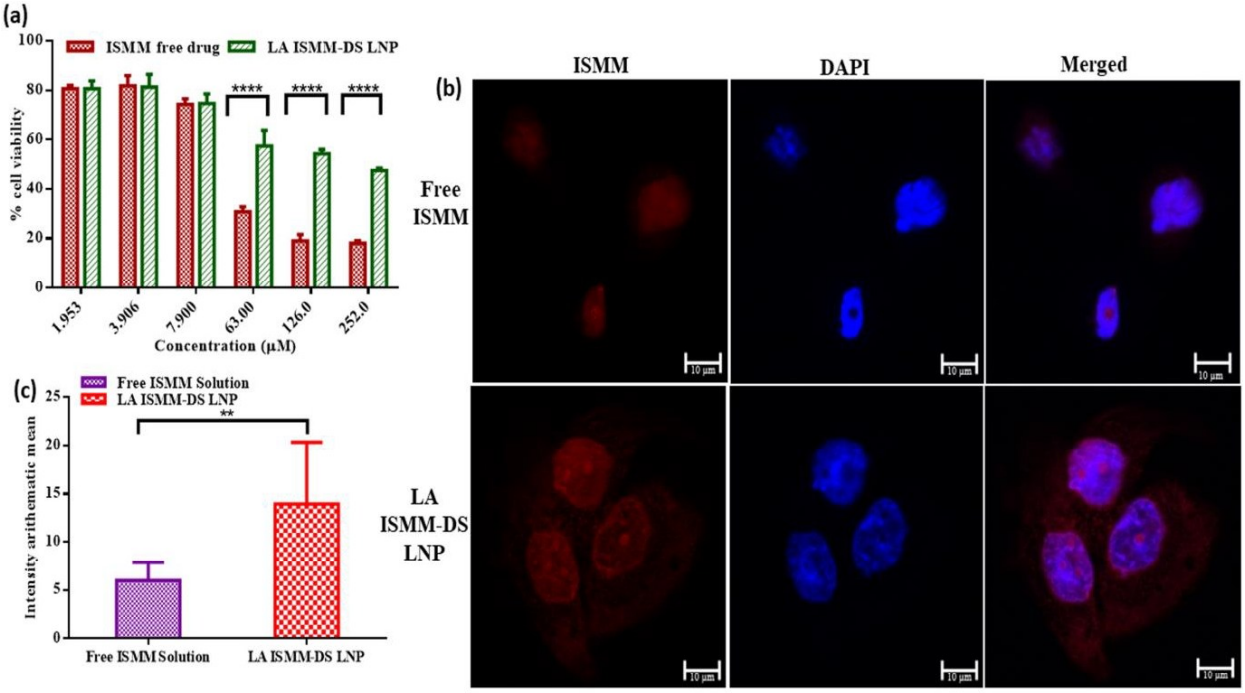

Figure 5.7 Cytotoxicity and cell uptake studies of LA ISMM-DS LNP. (a) MTT cytotoxicity studies in Vero cells (Each data represented as mean±SD, n=3; ** represents $p<0.01$ and **** represents $p<0.0001$, two-way ANOVA followed by Tukey's multiple comparison test) (b) Fluorescent micrographs of THP-1 macrophage cells after treatment with free ISMM and LA ISMM DS LNP counterstaining with DAPI at 1 h. (c) Quantitative cellular uptake of free ISMM and LA ISMM DS LNP in THP-1 macrophage cells (Each data represent mean ±SD, n=7; ** represents $p<0.05$, two-tailed unpaired t-test for cell uptake studies).

3.7 *In vivo* pharmacokinetics and biodistribution studies

ISMM equivalent/kg (30 mg) of free ISMM (group I) and LA ISMM-DS LNP (group II) were administered subcutaneously to elucidate LA potential of LA ISMM-DS LNP. The plasma ISMM concentration of free ISMM and LA ISMM-DS LNP was 268.8±47.13 ng/ml and 333.8±60.7 ng/ml respectively at 24 h and briskly reached below limit of detection in free ISMM administered rats. In contrast, protracted drug release was obtained upto 7 days in LA ISMM-DS LNP group (Figure 5.8(b)). To evaluate the pharmacokinetic (PK) of ISMM, the plasma ISMM concentration at each time-point was subjected to noncompartmental analysis (Table 5.3). The attribute of ISMM involving rapid organ biodistribution as

evidenced by its larger volume of distribution (V_z/F) and lower plasma ISMM level has been a major cause of concern for parasite relapse [4,14]. However, protracted plasma concentration of drugs in LA ISMM-DS LNP group until 7 days resulted in increased $AUC_{0-\infty}$ and $MRT_{0-\infty}$ by 3.0-folds and 4.5-folds, respectively in comparison with free ISMM group. Furthermore, an increase in V_z/F by 1.42-folds could be due to differentiated secondary immune cell depot in individual organs. Additionally, PBMC were isolated from blood at day 7 and ISMM concentration was determined revealing 68.4±19.0 ng/ml ISMM concentration in LA ISMM-DS LNP group as against ISMM concentration below the limit of detection in free ISMM group (Figure 5.8(c)) which confirmed the secondary depot in immune cells upon SC administration of ISMM-DS LNP. These results corroborate with observations from cell-uptake studies which showed enhanced cellular uptake in THP-I macrophage-like cells of LA ISMM-DS LNP compared with free ISMM. The increase in apparent terminal phase half-life ($t_{1/2}$) by 4.2-folds ensued from decreased clearance (CL/F) by 4.2-folds of LA ISMM-DS LNP compared with free ISMM. Lower initial plasma concentration of 229.3±42.8 ng/ml in group II when compared with group I (540.5±114.0 ng/ml) could be attributed to the characteristic slow release of ISMM from LA ISMM-DS LNP depot. Similar reports were established for hydrophilic antiretrovirals including tenofovir (M.W.:287.21, log P: -1.6, water solubility: 13.4 mg/ml) and emtricitabine (M.W.:247.25, Log P:-0.6, water solubility: 112 mg/ml) LA nanoformulation [50–52] and emtricitabine LA nanoformulation [53] with protracted drug release upto 14 and 7 days respectively when encapsulated into PLGA nanoparticles.

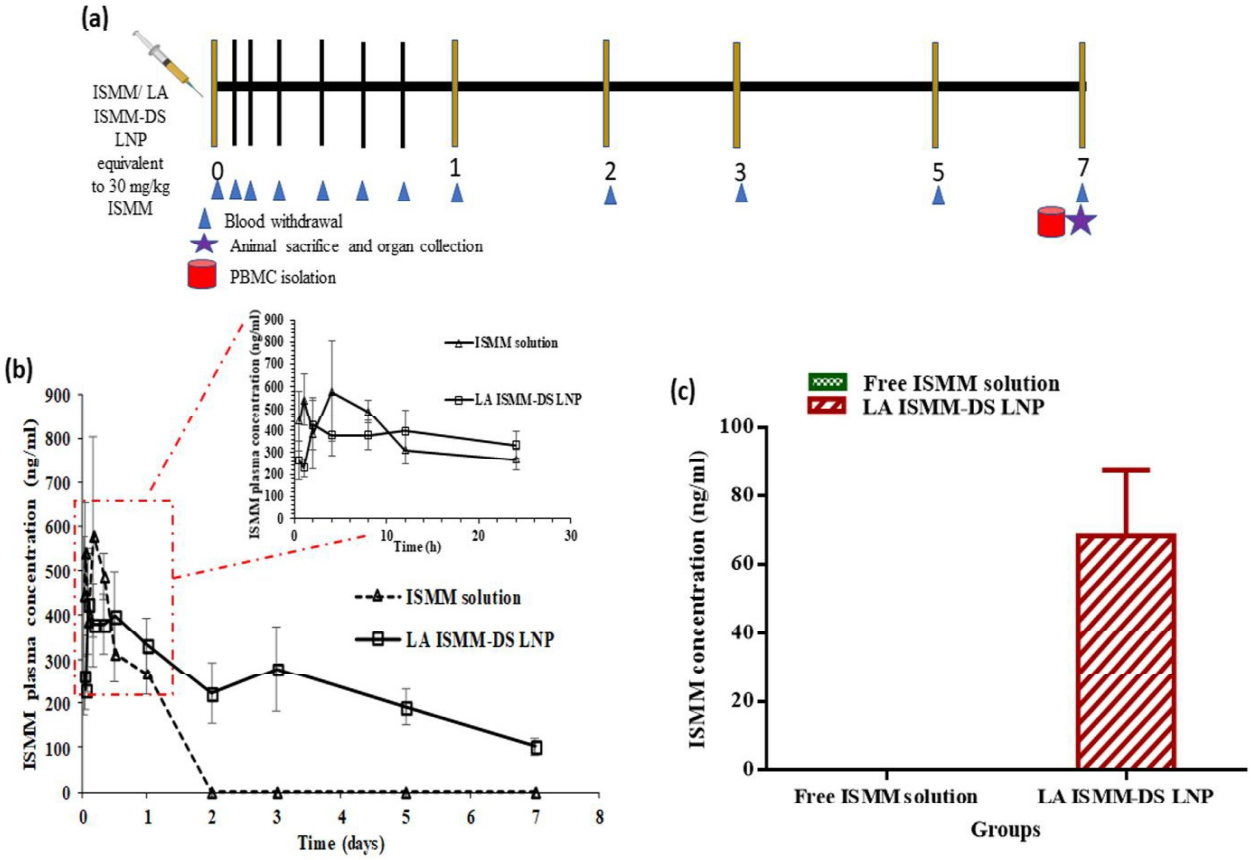

Figure 5.8 *In vivo* pharmacokinetic studies (a) Pharmacokinetic paradigm. (b) Pharmacokinetic profile of free ISMM and LA ISMM-DS LNP determined upto 7 days upon subcutaneous administration in male Wistar rats. (c) Concentration of LA ISMM-DS LNP determined at day 7 in isolated PBMC from male Wistar rat blood.

Table 5.3 Plasma noncompartmental PK parameters obtained from Phoenix WiNonlin software (version 2.1) for Wistar rats administered free ISMM and LA ISMM-DS LNP subcubtaneously

Parameter	**Results**	
	Free ISMM	ISMM-DS LNP
$AUC_{0-\infty}$ (h.ng/ml)***	17545.6±4527.1	53545.5±2516.5
$t_{1/2}$ (h)$^{\$}$	19.5±5.8	82.6±22.5
Vz/F (L/Kg)*	48016.8±5893.8	68428.3±19409.2
Cl/F$^{\$}$	2011.1±411.0	564.3±28.9
$MRT_{0-\infty}$$^{\$}$	30.1±8.7	134.9±30.0

Data represented as mean±SEM (n=4)

Biodistribution studies revealed the accumulation of ISMM in various reticuloendothelial system (RES) and non-RES organs in the order of liver>spleen>kidneys>lymph node>lungs on day 7. Insufficient plasma concentration obtained in the free ISMM group despite its

presence in primary depot could be due to the inherent trait of quick biodistribution within 10 min and the elimination of free ISMM [4]. Whereas, LA ISMM-DS LNP caused prolonged plasma and tissue concentration due to the relocation of ISMM depot into infiltered immune cells (secondary depot) from the injection site (primary depot). The results were in congruence with visual observation of the depot site in each animal of free ISMM and LA ISMM-DS LNP group at 72 h with evident depot pocket due to infiltered immune cells (secondary depot). The amount of ISMM was 2.9-, 4.2- and 2.0-folds higher in RES organs like liver (Kupffer cells), spleen (spleenotropic macrophages and 15% T-lymphocytes), and lymph nodes (75% T-lymphocytes), respectively in LA ISMM-DS LNP group which could be a repercussion of LA ISMM-DS LNP carriage into the lymphatic vessel by secondary depot cells; sequestration into the lymph node and steady transfer into systemic circulation preceded via thoracic duct (Figure 5.9). Furthermore, a significantly higher amount of ISMM in RES and non-RES organs would be an aftermath of increased Vz/F in LA ISMM-DS LNP group as against the free ISMM group. Thus, protracted week-long ISMM plasma drug concentration attained through LA ISMM-DS LNP would lead to reduced dosing frequency compared to free ISMM which would impel in reduced complications associated with subcutaneous administration of free ISMM. Furthermore, ISMM is majorly used against *T. evansi* infection which despite being hemoprotozoa; showed its existence in visceral forms in organs including liver, kidney, lungs, and cerebrum [54]. Therefore, prolonged primary (injection site) and secondary (immune cells and organs) depot would be of enormous value for treatment and pre-exposure prophylaxis against trypanosomiasis.

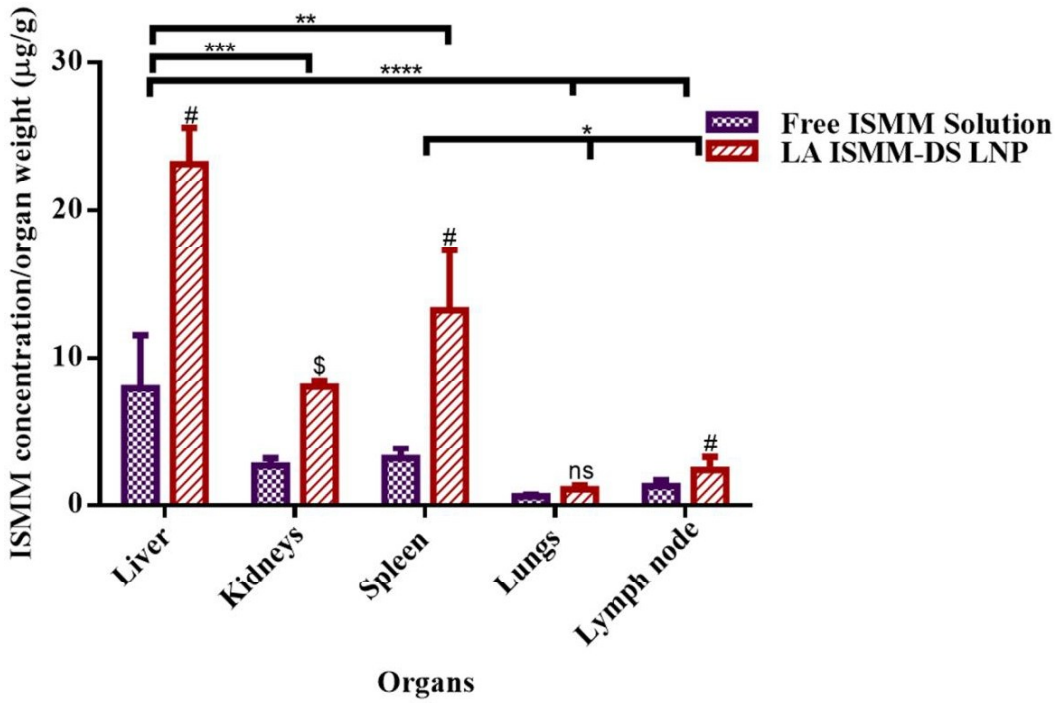

Figure 5.9 *In vivo* biodistribution profile of free ISMM and LA ISMM-DS LNP at day 7 in liver, kidneys, spleen, lungs, lymph node, and injection site upon subcutaneous administration. (Data represented as mean±SEM, n=4, **** represents $p<0.0001$,*** represents $p<0.001$, ** represents 0.01 and * represens $p<0.05$ by two-way multiple comparison ANOVA while, # represents $p<0.05$, $ represents $p<0.001$, versus free ISMM solution group of organ by student t-test)

4. Conclusion

The current study involved the development of LA solid lipid nanoparticles for the charged hydrophilic anti-trypanosomal drug (ISMM) which was unfledged until now. Furthermore, it divulges the role of anionic complexing agents in modulating the solubility and hydrophobicity of cationic moieties; thereby, elevating drug loading for drugs with a prerequisite of high dose. It ramified the significance of molecular weight, log P, and polar surface area of anionic complexing agents for pertinent selection in the formation of HIC. The sustained *in vitro* drug release for 24 h mimicked the *in vivo* scenario of ISMM-DS LNP after traversing the lymphatic system and draining into the circulatory system. While, the potential of secondary immune cell depot genesis by ISMM-DS LNP was confirmed *in vitro*

in THP-1 macrophage-like cells and *in vivo* depicting significant accumulation of ISMM-DS LNP in PBMC at day 7 upon subcutaneous administration. The ISMM-DS LNP depicted enormous pre-clinical success with protracted drug release in plasma upto 7 days for ISMM; which otherwise cause the least plasma retention ability. Furthermore, enhanced target tissue accumulation was accomplished with SC administration of ISMM-DS LNP depicting secondary tissue depot. To conclude, developed platform technology would be a boon for long-term prophylaxis and treatment of trypanosomiasis.

References

[1] Isometamidium chloride, (n.d.). https://pubchem.ncbi.nlm.nih.gov/compound/Isometamidium-chloride (accessed August 1, 2020).

[2] L.D.. Kinabo, J.A.. Bogan, The pharmacology of isometamidium, J.Vet. Pharmcol. Ther. 11 (1988) 233–245.

[3] G.A. Murilla, R.E. Mdachi, W. Karanja, Pharmacokinetics, bioavailability and tissue residues of [14C] isometamidium in non-infected and Trypanosoma congolense-infected Boran cattle, Acta Trop. 61 (1996) 277–292.

[4] Isometamidium, (n.d.). http://www.inchem.org/documents/jecfa/jecmono/v25je10.htm (accessed August 1, 2020).

[5] Z.Q. Zhang, C. Giroud, T. Baltz, In vivo and in vitro sensitivity of Trypanosoma evansi and T . equiperdum to diminazene, suramin, MelCy, quinapyramine and isometamidium, Acta Trop. 50 (1992) 101–110.

[6] F. Giordani, L.J. Morrison, T.I.M.G. Rowan, H.P.D.E. Koning, M.P. Barrett, The animal trypanosomiases and their chemotherapy : a review, Parasitology. 143 (2016)

1862–1889. doi:10.1017/S0031182016001268.

[7] K. Prayag, D.H. Surve, A.T. Paul, S. Kumar, A.B. Jindal, Nanotechnological interventions for treatment of trypanosomiasis in humans and animals, Drug Deliv. Transl. Res. 10 (2020) 945–961.

[8] African Animal Trypanosomiasis, (2018) 1–8. http://www.cfsph.iastate.edu/Factsheets/pdfs/trypanosomiasis_african.pdf (accessed August 1, 2020).

[9] Z. Bengaly, S.H. Vitouley, M.B. Somda, A. Zongo, A. Têko-agbo, G. Cecchi, Y. Adam, I. Sidibé, B. Bayala, A. Marie, G. Belem, J. Van Den Abbeele, V. Delespaux, Drug quality analysis of isometamidium chloride hydrochloride and diminazene diaceturate used for the treatment of African animal trypanosomosis in West Africa, BMC Vet. Res. 14 (2018) 1–8.

[10] Isometamidium chloride, Food Agric. Organ. United Nations. (n.d.). http://www.fao.org/fileadmin/user_upload/vetdrug/docs/41-2-isometamidium_chloride.pdf.

[11] L. Griffin, E.W. Allonby, The economic effects of Trypanosomiasis in sheep and goats at a range research station in Kenya, Trop. Anim.Hlth.Prod. 11 (1979) 127–132.

[12] L.L. Logan, J.T. Goodwin, S. Tembely, T.M. Craig, Maintaining Zebu Maure cattle in a tsetse infested area of Mali, Trop. Anim.Hlth.Prod. 16 (1984) 1–12.

[13] P.W.. Kanyari, E.W. Allonby, A.J. Wilson, W.K. Munyua, Some economic effects on trypanosomiasis in goats, Trop. Anim.Hlth.Prod. 15 (1983) 153–160.

[14] E.O. Mungube, H.S. Vitouley, E. Allegye-cudjoe, O. Diall, Z. Boucoum, B. Diarra, Y. Sanogo, T. Randolph, B. Bauer, K. Zessin, Detection of multiple drug-resistant

Trypanosoma congolense populations in village cattle of south-east Mali, Parasit. Vectors. 5 (2012) 1–9.

[15] S. Singh, M. Chopra, N. Dilbaghi, B.K. Manuja, S. Kumar, R. Kumar, N.S. Rathore, S.C. Yadav, A. Manuja, Synthesis and evaluation of isometamidium-alginate nanoparticles on equine mononuclear and red blood cells, Int. J. Biol. Macromol. 92 (2016) 788–794. doi:10.1016/j.ijbiomac.2016.07.084.

[16] B. Diarra, O. Diall, S. Geerts, P. Kageruka, Y. Lemmouchi, E. Schacht, M.C. Eisler, P. Holmes, Field Evaluation of the Prophylactic Effect of an Isometamidium Sustained-Release Device against Trypanosomiasis in Cattle, Antimicrob. Agents Chemother. 42 (1998) 1012–1014.

[17] D.H. Surve, A.B. Jindal, Recent advances in long-acting nanoformulations for delivery of antiretroviral drugs, J. Control. Release. 324 (2020) 379–404. doi:10.1016/j.jconrel.2020.05.022.

[18] Y.H. Song, E. Shin, H. Wang, J. Nolan, S. Low, D. Parsons, S. Zale, S. Ashton, M. Ashford, M. Ali, D. Thrasher, N. Boylan, G. Troiano, A novel in situ hydrophobic ion paring (HIP) formulation strategy for clinical product selection of a nanoparticle drug delivery system, J. Control. Release. 229 (2016) 106–119. doi:10.1016/j.jconrel.2016.03.026.

[19] B. Devrim, A. Bozkır, Design and Evaluation of Hydrophobic Ion-Pairing Complexation of Lysozyme with Sodium Dodecyl Sulfate for Improved Encapsulation of Hydrophilic Peptides / Proteins by Lipid-Polymer Hybrid Nanoparticles Nanomedicine & Nanotechnology, J. Nanomed. Nanotechnol. 6 (2015) 1–5. doi:10.4172/2157-7439.1000259.

[20] M. Tadele, S.M. Abay, E. Makonnen, A. Hailu, Leishmania donovani Growth

Inhibitors from Pathogen Box Compounds of Medicine for Malaria Venture, Drug Des. Devel. Ther. 14 (2020) 1307–1317.

[21] K.S. Joshy, S. Snigdha, N. Kalarikkal, L.A. Pothen, S. Thomas, Gelatin modified lipid nanoparticles for anti retroviral drug delivery, Elsevier Ireland Ltd, 2017. doi:10.1016/j.chemphyslip.2017.07.002.

[22] H.L. Wong, R. Bendayan, A.M. Rauth, X.Y. Wu, Development of solid lipid nanoparticles containing ionically complexed chemotherapeutic drugs and chemosensitizers, J. Pharm. Sci. 93 (2004) 1993–2008. doi:10.1002/jps.20100.

[23] A. Pourjavadi, S.S. Amin, S.H. Hosseini, Delivery of Hydrophobic Anticancer Drugs by Hydrophobically Modified Alginate Based Magnetic Nanocarrier, Ind. Eng. Chem. Res. 57 (2018) 822–832. doi:10.1021/acs.iecr.7b04050.

[24] C. Dumont, S. Bourgeois, H. Fessi, P. Dugas, V. Jannin, In-vitro evaluation of solid lipid nanoparticles: Ability to encapsulate , release and ensure effective protection of peptides in the gastrointestinal tract, Int. J. Pharm. 565 (2019) 409–418. doi:10.1016/j.ijpharm.2019.05.037.

[25] Docusate sodium, (n.d.). https://www.drugbank.ca/salts/DBSALT001500 (accessed August 1, 2020).

[26] Sodium alginate (FDB019541), (n.d.). https://foodb.ca/compounds/FDB019541 (accessed August 1, 2020).

[27] Dextran, (n.d.). https://pubchem.ncbi.nlm.nih.gov/compound/Dextran (accessed August 1, 2020).

[28] K.D. Ristroph, R.K. Prud, Hydrophobic ion pairing: encapsulating small molecules , peptides , and proteins into nanocarriers, Nanoscale Adv. 1 (2019) 4207–4237.

doi:10.1039/c9na00308h.

[29] B. Shah, D. Khunt, H. Bhatt, M. Misra, H. Padh, Application of quality by design approach for intranasal delivery of rivastigmine loaded solid lipid nanoparticles: Effect on formulation and characterization parameters, Eur. J. Pharm. Sci. 78 (2015) 54–66. doi:10.1016/j.ejps.2015.07.002.

[30] A. Siddiqui, A. Alayoubi, Y. El-malah, S. Nazzal, Modeling the effect of sonication parameters on size and dispersion temperature of solid lipid nanoparticles (SLNs) by response surface methodology (RSM), Pharm. Dev. Technol. 7450 (2013) 1–5. doi:10.3109/10837450.2013.784336.

[31] C. Kriegel, M. Festag, R.S.K. Kishore, D. Roethlisberger, G. Schmitt, Pediatric Safety of Polysorbates in Drug Formulations, Children. 7 (2020) 1–12.

[32] R. Yang, R. Gao, F. Li, H. He, X. Tang, The influence of lipid characteristics on the formation , in vitro release , and in vivo absorption of protein-loaded SLN prepared by the double emulsion process, Drug Dev. Ind. Pharm. 37 (2011) 139–148. doi:10.3109/03639045.2010.497151.

[33] M.H. Aburahma, S.M. Badr-eldin, Compritol 888 ATO: a multifunctional lipid excipient in drug delivery systems and nanopharmaceuticals, Expert Opin. (2014) 1–19.

[34] N. Abdel, H. Abou, A. Ahmed, R. Mohamed, F. Ahmed, M. Abd, E. El-massik, N. Ahmed, A novel nasal almotriptan loaded solid lipid nanoparticles in mucoadhesive in situ gel formulation for brain targeting: Preparation , characterization and in vivo evaluation, Int. J. Pharm. 548 (2018) 609–624. doi:10.1016/j.ijpharm.2018.07.014.

[35] J. Qing, S. Zhen, W. Yi, A. Wen, W. Ni, X. Jing, Modification and stabilizing effects

of PEG on resveratrol-loaded solid lipid nanoparticles, J. Iran. Chem. Soc. 13 (2016) 881–890. doi:10.1007/s13738-015-0803-9.

[36] M.K. Lee, M.Y. Kim, S. Kim, J. Lee, Cryoprotectants for Freeze Drying of Drug Nano-Suspensions: Effect of Freezing Rate, J. Pharamceutical Sci. 98 (2009) 4808–4817. doi:10.1002/jps.

[37] W. Abdelwahed, G. Degobert, S. Stainmesse, H. Fessi, Freeze-drying of nanoparticles: Formulation, process and storage considerations, Adv. Drug Deliv. Rev. 58 (2006) 1688–1713. doi:10.1016/j.addr.2006.09.017.

[38] M.A. Moretton, D.A. Chiappetta, A. Sosnik, Cryoprotection-lyophilization and physical stabilization of rifampicin-loaded flower-like polymeric micelles, J.R.Soc. Interface. 9 (2012) 487–502.

[39] S. Mandal, G. Kang, P. Kumar, Y. Zhou, W. Fan, Q. Li, C.J. Destache, Nanoencapsulation introduces long-acting phenomenon to tenofovir alafenamide and emtricitabine drug combination: A comparative pre-exposure prophylaxis efficacy study against HIV-1 vaginal transmission, J. Control. Release. 294 (2019) 216–225. doi:10.1016/j.jconrel.2018.12.027.

[40] J. Kraft, L. McConnachie, J. Koehn, L. Kinman, J. Sun, A. Collier, C. Collins, D. Shen, R. Ho, Mechanism-based pharmacokinetic (MBPK) models describe the complex plasma kinetics of three antiretrovirals delivered by a long-acting anti-HIV drug combination nanoparticle formulation, J. Control. Release. 275 (2018) 229–241. doi:10.1016/j.jconrel.2018.02.003.

[41] M. Yayeh, S. Dagnachew, M. Tilahun, A. Melaku, T. Mitiku, M. Yesuf, Z. Seyoum, H. Kefyalew, Comparative experimental studies on Trypanosoma isolates in mice and response to diminazene aceturate and isometamidium chloride treatment, Heliyon. 4

(2018) 1–18. doi:10.1016/j.heliyon.2018.e00528.

[42] J. Wagner, G. DeLoach, Some Effects of the Trypanocidal Drug Isometamidium on Encapsulation in Bovine Carrier Erythrocytes, Biotechnol. Appl. Biochem. 10 (1988) 447–453.

[43] S.M. Alsanosi, C. Skiffington, S. Padmanabhan, Chapter 17-Pharmacokinetic Pharmacogenomics, in: Handb. Pharmacogenomics Stratif. Med., 2014: pp. 341–364.

[44] E. Lozano, E. Herraez, O. Briz, V.S. Robledo, J. Hernandez-iglesias, A. Gonzalez-hernandez, J.J.G. Marin, Role of the Plasma Membrane Transporter of Organic Cations OCT1 and Its Genetic Variants in Modern Liver Pharmacology, Biomed Res. Int. (2013) 1–13.

[45] N.C. Ammerman, M. Beier-Sexton, A.F. Abdu, Growth and maintenance of Vero cell lines, Curr Protoc Microbiol. (2008) 1–10. doi:10.1002/9780471729259.mca04es11.Growth.

[46] A. Owen, S. Rannard, Strengths, weaknesses, opportunities and challenges for long acting injectable therapies: Insights for applications in HIV therapy, Adv. Drug Deliv. Rev. 103 (2016) 144–156. doi:10.1016/j.addr.2016.02.003.

[47] S. Perazzolo, L.M. Shireman, L.A. Mcconnachie, J.C. Kraft, D.D. Shen, R.J.Y. Ho, Three HIV Drugs, Atazanavir, Ritonavir, and Tenofovir, Coformulated in Drug-Combination Nanoparticles Exhibit Long-Acting and Lymphocyte-Targeting Properties in Nonhuman Primates, J. Pharmceutical Sci. 101 (2018) 1–10. doi:10.1016/j.xphs.2018.07.032.

[48] T. Berg, T. Hegelund-myrbäck, J. Öckinger, X. Zhou, M. Brännström, M. Hagemann-jensen, V. Werkström, J. Seidegård, J. Grunewald, M. Nord, L. Gustavsson, OCTN2 ,

in epithelial and immune cells in the lung of COPD and healthy individuals, Respir. Res. 19 (2018) 1–13.

[49] L. Arana, L. Bay, L.I. Sarasola, M. Berasategi, S. Ruiz, I. Alkorta, Solid Lipid Nanoparticles Surface Modification Modulates Cell Internalization and Improves Chemotoxic Treatment in an Oral Carcinoma Cell Line, Nanomaterials. 9 (2019) 1–17. doi:10.3390/nano9030464.

[50] Tenofovir, (n.d.). https://pubchem.ncbi.nlm.nih.gov/compound/Tenofovir (accessed August 1, 2020).

[51] Emtricitabine, (n.d.). https://pubchem.ncbi.nlm.nih.gov/compound/Emtricitabine#section=Chemical-and-Physical-Properties (accessed August 2, 2020).

[52] S. Mandal, G. Kang, P. Kumar, Y. Zhou, W. Fan, Q. Li, C.J. Destache, Nanoencapsulation introduces long-acting phenomenon to tenofovir alafenamide and emtricitabine drug combination : A comparative pre- exposure prophylaxis e ffi cacy study against HIV-1 vaginal transmission, J. Control. Release. 294 (2019) 216–225. doi:10.1016/j.jconrel.2018.12.027.

[53] I.M. Ibrahim, D. Soni, H.E. Gendelman, Synthesis and characterization of a long-acting emtricitabine prodrug nanoformulation, Int. J. Nanome. 14 (2019) 6231–6247.

[54] M. Singh, B.L.D. Singla, H.K. Ashuma, Pathological studies on experimental Trypanosoma evansi infection in Swiss albino mice, J. Parasit Dis. 36 (2012) 260–264. doi:10.1007/s12639-012-0120-5.